# A temperature prediction-correction method for estimating surface soil heat flux from soil temperature and moisture data

YANG Kun[1†] & WANG JieMin[2]

[1] Institute of Tibetan Plateau Research, Chinese Academy of Sciences, Beijing 100085, China;
[2] Cold and Arid Regions Environmental and Engineering Research Institute, Chinese Academy of Sciences, Lanzhou 730000, China

**Surface soil heat flux is a component of surface energy budget and its estimation is needed in land-atmosphere interaction studies. This paper develops a new simple method to estimate soil heat flux from soil temperature and moisture observations. It gives soil temperature profile with the thermal diffusion equation and, then, adjusts the temperature profile with differences between observed and computed soil temperatures. The soil flux is obtained through integrating the soil temperature profile. Compared with previous methods, the new method does not require accurate thermal conductivity. Case studies based on observations, synthetic data, and sensitivity analyses show that the new method is preferable and the results obtained with it are not sensitive to the availability of temperature data in the topsoil. In addition, we pointed out that the soil heat flux measured with a heat-plate can be quite erroneous in magnitude though its phase is accurate.**

Surface soil heat flux is an important component of the surface energy budget, and its estimation is involved in almost all analyses of atmospheric boundary layer (ABL) experiments and land surface-atmosphere interaction studies. Due to solar heating, the topsoil usually experiences dramatic diurnal changes in soil temperature and heat flux. Accordingly, soil heat flux exponentially decays with increasing soil depth[1]. Soil heat flux can be measured with a heat-plate. Except very few cases[2], a heat-plate is usually buried at a certain depth, and thus its measurement does not represent the surface soil heat flux. On the other hand, soil temperature and moisture profiles have been measured by many ABL stations, automatic weather stations (AWS), and ecological observational networks. It is a basic approach to derive soil heat flux by integrating these data based on the thermal diffusion equation. For instance, Tanaka et al.[3] integrated soil moisture and temperature data to calculate soil heat flux at Anduo site on the Tibetan Plateau; Li et

al.[4] developed an integral method to calculate the heat flux at different layers by using soil temperature profile data. Other types of soil heat flux estimates are based on the phase delay of soil temperature with increasing depth or the decay of its amplitude with increasing depth. Horton et al.[5] and Mo et al.[6] compared several such methods and concluded that numerical and harmonic methods had better accuracy. Fan et al.[7] and Gao et al.[8,9] presented new ideas to take both conduction and convection processes into the calculation of soil heat flux. These methods assume a vertically homogeneous soil (constant thermal conductivity or diffusivity), or assume that the soil temperature in each layer follows a sine-curve diurnal variation, and then derive soil parameters (such as diffusivity) with temperature phase

and amplitude observations. These assumptions may be either far from the reality or difficult in practical application, thus inducing significant errors. In addition, some methods are based on empirical relationships between soil heat fluxes and net radiation[10]. The coefficients in these relationships can be spatially dependent, and the estimate has errors in the phase of soil heat fluxes. A review on soil heat flux calculation can be referred to Zhang et al.[11].

Based on the thermal diffusion equation, this paper develops a new method to calculate surface soil heat flux from soil temperature and moisture measurements. It does not require prior knowledge of soil thermal conductivity or diffusivity but can estimate soil heat flux with satisfied accuracy. It is reminded that the heat flux in a deep soil is far below the magnitude of surface soil heat flux, and thus its calculation method is different[12], which is beyond our objective and is not discussed in this paper.

# 1 Theory for calculating soil heat flux

The one-dimensional soil Thermal Diffusion Equation (TDE) is:

$$\frac{\partial \rho_s c_s T}{\partial t} = \frac{\partial G}{\partial z}, \tag{1}$$

$$G = \lambda_s \frac{\partial T}{\partial z}, \tag{2}$$

where $t$(s) is the time, $z$(m) the soil depth (positive if downward), $T$(K) the soil temperature, $\rho_s c_s$ ($J \cdot kg^{-1} \cdot K^{-1}$) the soil heat capacity, $\lambda_s$ ($W \cdot K^{-1} \cdot m^{-1}$) the soil thermal conductivity, and $G$($W \cdot m^{-2}$) the soil heat flux (positive if downward).

Integrating eq. (1) gives

$$G(z) = G(z_{ref}) + \int_{z_{ref}}^{z} \frac{\partial \rho_s c_s T(z)}{\partial t} dz. \tag{3}$$

Eq. (3) shows that the necessary conditions for estimating soil heat flux are: (1) The heat flux at a reference depth ($z_{ref}$), i.e. $G(z_{ref})$, (2) soil heat capacity, and (3) soil temperature profile. The soil heat capacity can be calculated by the following formulas[13]:

$$\rho_s c_s = \rho_{dry} c_{dry} + \rho_w c_w \theta, \tag{4a}$$

$$\rho_{dry} c_{dry} \approx (1 - \theta_{sat}) \times 2.1 \times 10^6 \quad J \cdot kg^{-1} \cdot K^{-1}, \tag{4b}$$

$$\rho_w c_w \approx 4.2 \times 10^6 \quad J \cdot kg^{-1} \cdot K^{-1}, \tag{4c}$$

where $\theta$($m^{-3} \cdot m^{-3}$) is the soil water content, $\theta_{sat}$

($m^{-3} \cdot m^{-3}$) the soil porosity, $\rho_{dry} c_{dry}$ ($J \cdot kg^{-1} \cdot K^{-1}$) the heat capacity of a dry soil, and $\rho_w c_w$ ($J \cdot kg^{-1} \cdot K^{-1}$) the heat capacity of liquid water. For a frozen soil, the heat capacity of frozen water should be taken into account[14].

Given temperature profile $T(z_i)$, the discretized form of eq. (3) is:

$$G = G(z_{ref}) +$$

$$\frac{1}{\Delta t} \sum_{z_{ref}}^{z} \left[ \rho_s c_s(z_i, t + \Delta t) T(z_i, t + \Delta t) - \rho_s c_s(z_i, t) T(z_i, t) \right] \Delta z.$$

$$\tag{5}$$

The heat flux $G(z_{ref})$ can be measured directly by a heat-plate. Alternatively, if the reference level $z_{ref}$ is so deep that $G(z_{ref})$ is much less than surface soil heat flux, it is acceptable to assume $G(z_{ref}) \approx 0$. The heat capacity can be calculated from soil water content and soil porosity that can be easily measured. Therefore, the key issue to calculate soil heat flux is how to make a reliable temperature profile from limited observations. Some studies smoothed temperature profile using linear interpolation or cubic splines[15]. In this study, we presented a new method.

# 2 New Method

## 2.1 Solution of the thermal diffusion equation

Soil temperature can be calculated by TDE (eq. (1)). The discretized model domain is shown in Figure 1. Because soil temperature varies dramatically in the top soil, we used stretching computational nodes, i.e., a layer near the surface is thinner than that in the deep soil. The layer thickness is given by

$$\Delta z_1 = D\left(e^{\xi} - 1\right)/(e^{n\xi} - 1), \tag{6a}$$

$$\Delta z_i = e^{\xi(i-1)} \Delta z_1, \tag{6b}$$

where $D$ is the model domain, and $\xi$ is a stretching parameter. If $\xi = 0$, the node spacing becomes uniform.

The discretized TDE form can be represented by a tridiagonal system:

For the 1st node

$$T_1 = T_{sfc}. \tag{7a}$$

For the $i$th node

$$A_i T_i^{t+\Delta t} = B_i T_{i+1}^{t+\Delta t} + C_i T_{i-1}^{t+\Delta t} + D_i, \tag{7b}$$

where $A_i = \frac{1}{2} \rho_s c_{s,i} (\Delta z_{i-1} + \Delta z_i) + \frac{\lambda_{s,i-1} \Delta t}{\Delta z_{i-1}} + \frac{\lambda_{s,i} \Delta t}{\Delta z_i}$, $B_i =$

$\frac{\lambda_{s,i} \Delta t}{\Delta z_i}$, $C_i = \frac{\lambda_{s,i-1} \Delta t}{\Delta z_{i-1}}$, $D_i = \frac{1}{2} \rho_s c_{s,i} (\Delta z_{i-1} + \Delta z_i) T_i^t$.
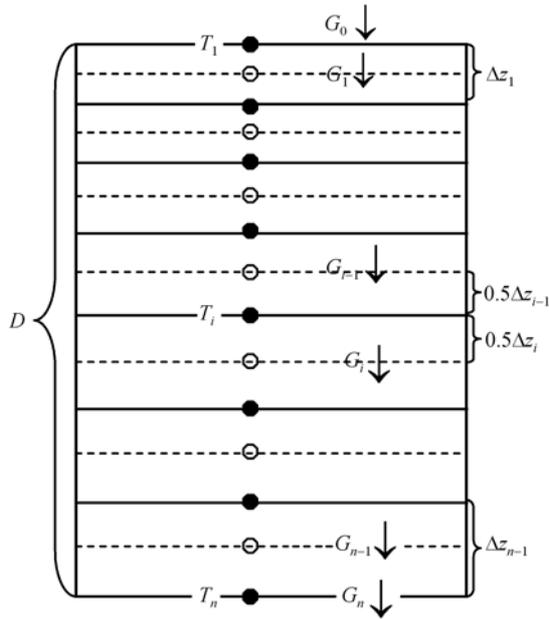
**Figure 1** A sketch of discretized model domain for the thermal diffusion equation. Solid dots denote temperature nodes. Circles denote flux nodes. Solid node 1 is at the surface and node $n$ at the bottom. $D$ is the model domain. Layer thickness is calculated according to eq. (6).

For the $n$th node

$$T_n = T_{bot}. \qquad (7c)$$

Solving the equation set requires two boundary conditions: surface skin temperature ($T_{sfc}$) and soil temperature at the bottom ($T_{bot}$).

### 2.2 Correction to temperature profile

To solve eq. (7) requires soil thermal conductivity, which depends on soil texture and soil water content. Because of the complexity in reality, it is not easy to measure or derive representative values of soil parameters. For simplicity, we assume a constant thermal conductivity in eq. (7). The computed temperature, therefore, deviates from observation; however, the bias is usually much less than the change of soil temperature. In other words, the temperature computed from TDE has accounted for the major part of the soil temperature change. The temperature bias, a minor part of the temperature change, is simply corrected as follows: first, the bias $\Delta T_k$ is calculated with $\Delta T_k = T_{k,obs} - T_{k,TDE}$ (Herein, $k$ is the observational point, $T_{k,obs}$ is the observed temperature, and $T_{k,TDE}$ is the solution of eq. (7); second, the bias is linearly interpolated from observing points ($\Delta T_k$) into computational nodes ($\Delta T_i$); finally, the temperature profile $T_{i,TDE}$ is corrected with $T_i = T_{i,TDE} + \Delta T_i$.

### 2.3 Heat flux calculation

If the model domain is deep enough, the heat flux at the lower bound of the model domain can be neglected, i.e., $G(z_{ref}) \approx 0$. We recommend extending the model domain to the deepest observational point, as the computational cost is low. Integrating eq. (5) from the bottom to the surface, one can obtain soil heat fluxes at all layers.

The above-introduced method is simple and can be easily realized. For the convenience of description, the new method is named after TDEC (Thermal Diffusion Equation and Correction) in the remaining sections.

## 3 Comparison and validation

Using data collected at the GAME-Tibet Anduo (or Amdo) site, this section investigates the reliability of TDEC. Anduo was a comprehensive station of GEWEX (Global Energy and Water Cycle Experiment) Asian Monsoon Experiment (GAME)-Tibet[16]. It was located at (32.241°N, 91.635°E, altitude 4700 m) in the central Plateau. During 1998 IOP (Intensive Observing Period), high quality data of ABL profile, land surface variables, as well as soil temperature and moisture at this site were obtained. These data have been widely used to investigate land-atmosphere interactions and soil physical processes[3,10,17−20].

Table 1 lists the measurements relevant to this study. Among them, the measurement site of longwave radiation used for the conversion of ground surface temperature was collocated with the AWS (automatic weather station); the SMTMS (soil moisture and temperature measuring system) had a different footprint though not far from the AWS. In order to compare the computed heat fluxes with heat-plate measurements at AWS location, this study selected surface temperature, AWS three-level (5, 10 and 20 cm) temperatures, and SMTMS six-level (40, 60, 80, 100, 130 and 160 cm) temperatures to constitute the observed temperature profile; the soil moisture profile consists of SMTMS five-level (10, 20, 60, 100 and 160 cm) data. Surface temperature was converted from upward and downward longwave radiation components:

$$T_{sfc} = [(R_{lw}^{\uparrow} - (1-\varepsilon_g)R_{lw}^{\downarrow})/(\varepsilon_g\sigma)]^{1/4}, \qquad (8)$$

where the surface emissivity $\varepsilon_g = 0.98$, given empirically; the Stefan-Boltzmann constant $\sigma = 5.67 \times 10^{-8}$ W·m$^{-2}$·K$^{-4}$.

**Table 1** Surface and soil measurements at Anduo site of GAME-Tibet in 1998

|  | Variables | Depth (cm) | Sampling Frequency (h$^{-1}$) |
|---|---|---|---|
| Surface radiation | Downward long-wave | 0 | 2 |
|  | Upward long-wave | 0 | 2 |
| AWS | Soil temperature | 5, 10, 20 | 2 |
|  | Soil heat flux | 10, 20 | 2 |
| SMTMS | Soil temperature | 4, 20, 40, 60, 80, 100, 130, 160 | 1 |
|  | Soil moisture | 10, 20, 60, 100, 160 | 1 |

The soil at this site has a strong vertical heterogeneity. Yang et al.[21] used a sandwich-like structure to mimic the soil. The topsoil contains dense grass roots and organic matters, the deep soil is sandy, and the middle layer is a transitional layer. Soil porosity $\theta_{sat}$ was obtained through laboratory analysis. Soil heat capacity was calculated with the measured porosity and soil water content.

### 3.1 Sensitivity of soil thermal conductivity

Due to extreme difficulties in the measurement of soil thermal conductivity, it is assumed to be a constant in the TDEC method. At first, we should confirm that the heat flux estimated from TDEC is not sensitive to the assumed thermal conductivity. For comparisons with TDEC, soil heat flux was also calculated from TDE which makes no correction to temperature biases. Figure 2 shows the comparisons of heat fluxes at Anduo site, given different thermal conductivities (0.5 and 2.0 W·m$^{-1}$·k$^{-1}$), showing that the fluxes from TDEC are very similar (Figure 2(a)) even though the used

thermal conductivity values are very different. By contrast, the results of TDE are very sensitive to the thermal conductivity (Figure 2(b)). Similar results were found for fluxes at 10 and 20 cm. Therefore, it is the temperature correction that makes the heat flux estimated from TDEC not sensitive to the thermal conductivity. In all calculations below, the heat conductivity is set to be 1.0 W·m$^{-1}$·k$^{-1}$, if no additional statement is presented.

### 3.2 Comparison with heat-plate measurements

Figure 3(a) shows the observed and computed heat storage in the layer between 10 and 20 cm at Anduo site. The heat storage is the heat flux at 10 cm minus that at 20 cm, showing that the computed one is much larger than the observed one, though they are highly correlated with each other. Whether this is due to computational errors or observational errors will be discussed in the following.

First, TDEC is based on a physical equation, and the temperature measurements used were with a high-accuracy (0.1 K). Therefore, computational errors are mainly from the errors in computed heat capacity, including heat capacity of the dry soil and liquid water. Heat capacity of a dry soil depends on the soil porosity; the higher the porosity, the lower the heat capacity. Heat capacity of liquid water depends on soil water content; the lower the water content, the lower the heat capacity. At Anduo site, the soil porosity at 5 cm depth (about 0.61) was far greater than that at 20 cm depth (about 0.38)[21]; in response, observed soil water content at 4 cm (0.55 on average) was much greater than that at 20 cm (0.25 on average)[19]. In Figure 3(a), the heat
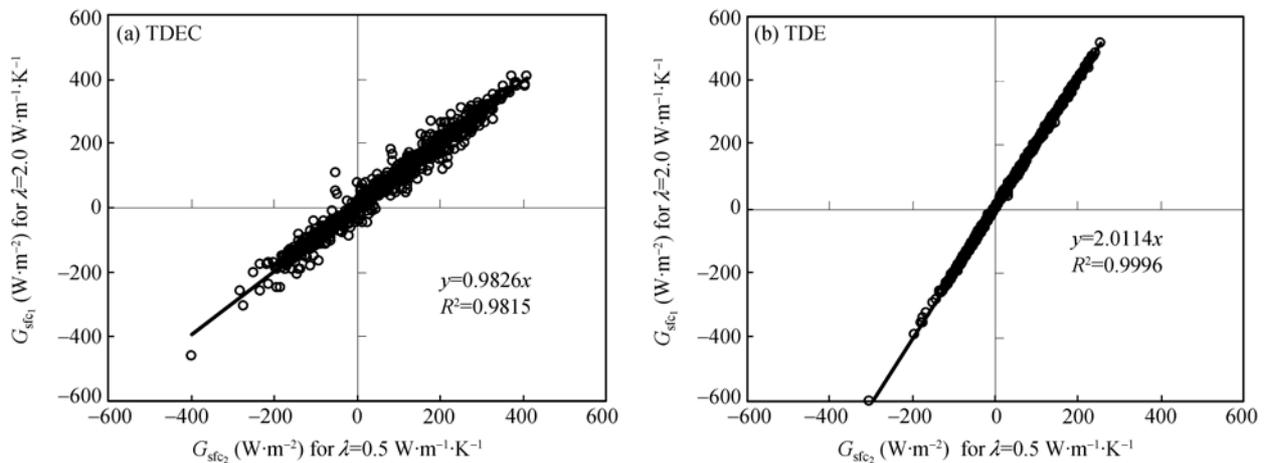


**Figure 2** Comparisons of surface soil heat fluxes at different thermal conductivities (X-axis: 0.5 W·m$^{-1}$·K$^{-1}$, Y-axis: 2.0 W·m$^{-1}$·K$^{-1}$) at Anduo site. (a) TDEC, and (b) TDE. The straight line is fit for the data.

ity at nodes within the 10−20 cm layer was linearly interpolated from the top soil and 20 cm depth. In order to estimate the upper and lower bounds of soil heat flux, we used the heat capacity of the top soil or that of 20 cm depth, respectively, to represent the heat capacity of the 10−20 cm layer and re-calculated the heat storage of the 10−20 cm layer. The results are shown in Figure 3(b) and (c), showing that the computed heat storage is more than twice the observed one, and therefore, the difference between the computed and the observed heat fluxes is not caused by computational errors. By contrast, this implies that the thermal conductivity of the heat-plate used at Anduo site (0.21 $W \cdot m^{-1} \cdot K^{-1}$) was much less than the soil heat conductivity, resulting in large measurement errors. Hence, the measured flux is not able to represent the exact flux at the measurement level and needs corrections[22,23]. We noted that some studies[3] directly utilized the measurement as a reference heat flux to integrate surface soil heat flux.

On the other hand, the sign and phase of heat flux measured by the heat-plate are undoubtedly accurate. Figure 4 shows the observed and calculated heat storage

within the 10−20 cm layer at Anduo site. For a better visualization, observed values were amplified and only 10 d (10−20 August, 1998) were shown. It is shown that the TDEC-calculated heat flux well follows the observed sign, phase, as well as dramatic change of the heat fluxes, indicating that TDEC has small errors in the phase of the estimated heat flux.

### 3.3 Validation of soil heat flux

In addition to its measurement errors in magnitude, a heat-plate cannot measure the 'surface' soil heat flux, and therefore, it is difficult to directly validate the soil heat fluxes from TDEC. In this section, we design a numerical twin-experiment to validate TDEC results in two steps.

Step 1: "True" (or "observation") values were produced by solving TDE (eq. (7)). The numerical model data are also called synthetic data. We made a data set similar to the observations at Anduo Site. The surface temperature and bottom temperature observed at Anduo site were the boundary conditions of eq. (7), the temperature was initialized with the observations on 1 August, 1998, and the heat capacity was calculated from
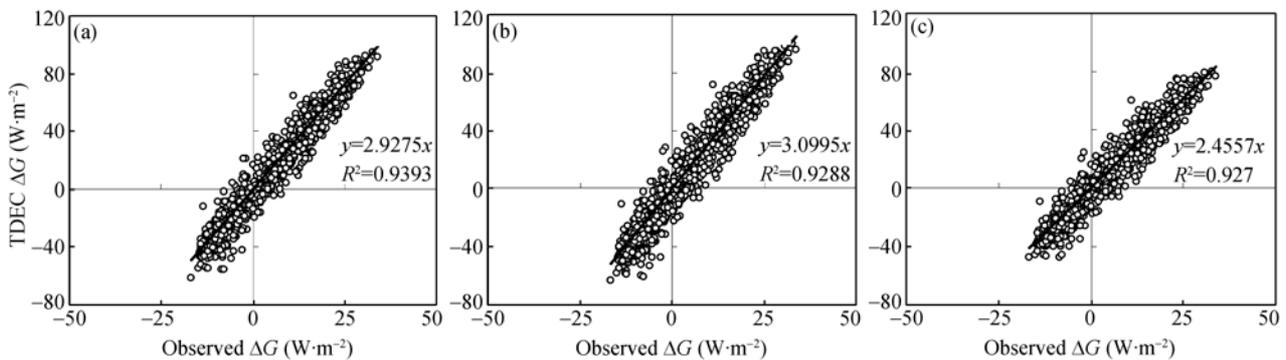


**Figure 3**  Observed and calculated heat storage within the 10−20 cm layer at Anduo site. X-axis: Heat-plate observed. Y-axis: TDEC calculated. In the calculation, heat capacity within the 10−20 cm layer is (a) interpolated from the top soil and 20 cm depth; (b) equal to that of the top soil; (c) equal to that of 20 cm depth. The straight line is fit for the data.
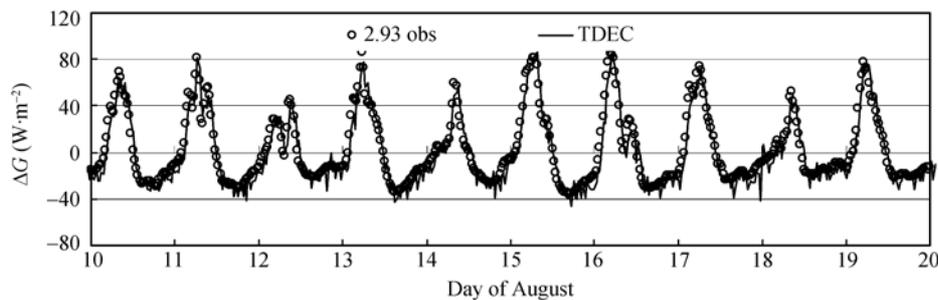


**Figure 4**  Observed and calculated heat storage within the 10−20 cm layer at Anduo site on 10−20 August, 1998. Observed values were amplified for a better visualization.

capacobserved soil water content. Temperature profile was given with eq. (7), and soil heat flux was then calculated according to eq. (5). The soil porosity was specified as 0.6, and the thermal conductivity was calculated by[21]

$$\lambda_s = \lambda_{dry} + (\lambda_{sat} - \lambda_{dry})\exp[0.36(1 - \theta_{sat}/\theta)], \quad (9a)$$

$$\lambda_{dry} = (170\rho_{dry} + 64.7)/(2700 - 947\rho_{dry}), \quad (9b)$$

$$\lambda_{sat} = 2.0, \quad (9c)$$

where the maximum thermal conductivity $\lambda_{sat} = 2.0 \text{ W} \cdot \text{m}^{-1} \cdot \text{K}^{-1}$ is an arbitrary value.

The numerical model produced data similar to those in Table 1, including temperature at multiple levels and heat fluxes at surface, 10 and 20 cm depths, with a sampling frequency of 30 min.

Step 2: Soil heat flux was calculated by TDEC. The temperature data from Step 1 was the input of TDEC, and the heat flux data from Step 1 were used for validation of TDEC result. It is worthy of noting that soil thermal conductivity in TDE (the forward model) of Step 1 varied with soil water content, while it was a constant (1 W$\cdot$m$^{-1}\cdot$K$^{-1}$) in TDEC (the inverse model) of Step 2.

Figure 5 shows that TDEC-estimated surface soil heat fluxes agree well with the "true" values, though the used thermal conductivity values in the forward and inverse models are quite different. Similar conclusions can be drawn from the comparisons of 10 and 20 cm depths (figure omitted).
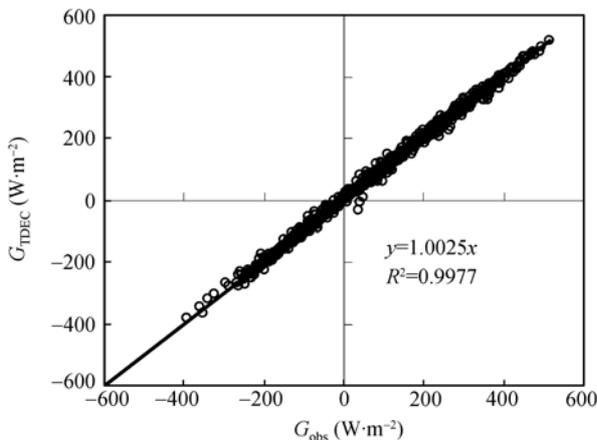


**Figure 5** Comparison between TDEC-derived surface soil heat fluxes and the "true" values in the twin-experiment. The straight line is fit for the data.

# 4 Comparison between TDEC method and LINEAR method

Heat fluxes can also be calculated based on linearly interpolated temperature profile (hereafter called LINEAR method). This section will compare the results of LINEAR and TDEC.

## 4.1 Comparison of results

Figure 6 shows comparisons of soil heat fluxes from TDEC and LINEAR at Anduo site. Panels ((a)−(c)) show the results for surface, 10, and 20 cm depths, respectively. It is clear that the fluxes from the two methods are highly correlated with each other, but the fluxes from TDEC are less than the ones from LINEAR by about 10%, during both daytime and nighttime. Similar results were obtained in the twin-experiment case (not shown). The following presents why LINEAR has a systematic negative bias.

Figure 7 shows observed and linearly interpolated temperature profiles in the daytime and the nighttime ($z_1$ and $z_2$ are thermometer-setting depths). To simplify the analysis, we assume that the heat capacity is independent of time and depth. Eq. (5) can be simplified as

$$G = G(z_{ref}) + \frac{\rho_s c_s}{\Delta t}\sum_{z_{ref}}^{z}[T(z_i, t + \Delta t) - T(z_i, t)]\Delta z. \quad (10)$$

Clearly, $\sum_{z_{ref}}^{z}[T(z_i, t + \Delta t) - T(z_i, t)]\Delta z$ denotes the area occupied by the two temperature profiles in Figure 7. It is equal to the area ($S_1$) occupied by horizontal dash lines if observed profiles are used, equalling the area ($S_2$) occupied by both horizontal and vertical dash lines if linearly interpolated profiles are used. Therefore, the error in soil heat fluxes caused by LINEAR,

$$\delta G = \frac{\rho_s c_s}{\Delta t}(S_2 - S_1), \quad (11)$$

i.e., the error is proportional to the area occupied by vertical dash lines. LINEAR would lead to both downward heat flux from the nighttime to daytime and upward heat flux from the daytime to nighttime over-estimated. In other words, LINEAR always results in over-estimates of surface soil heat flux.

## 4.2 Sensitivity of data availability in the topsoil

Above analyses were based on dense observations. This section will clarify how different the results of TDEC and LINEAR would be, if there were no observational data in the top several centimeters. For this purpose, we excluded temperature data at 5 cm depth, and re-calculated soil heat fluxes using TDEC and LINEAR, respectively. Figure 8 shows the differences in soil heat
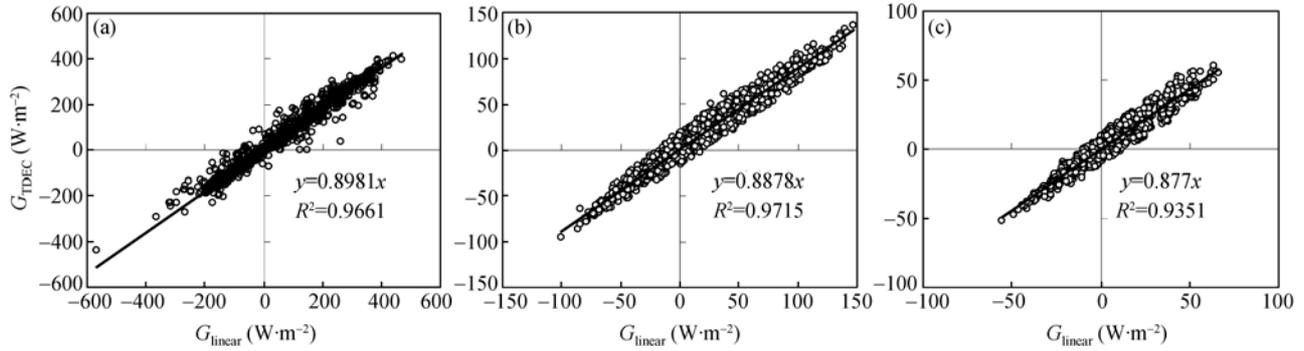
**Figure 6** Comparisons of heat fluxes from TDEC and LINEAR at Anduo site. Panels ((a)−(c)) show the results for surface, 10, and 20 cm depths, respectively.
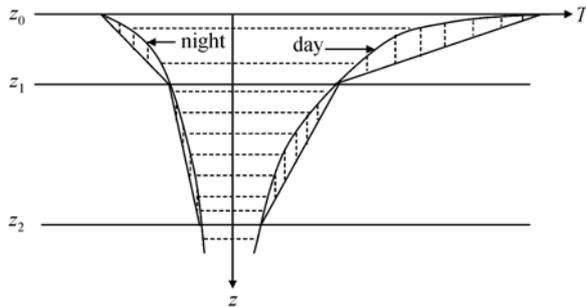


**Figure 7** Soil temperature profile in the daytime and the nighttime. $z_0$, $z_1$, and $z_2$ are observational depths. The area occupied by horizontal dash lines represents actual temperature change, while the area occupied by vertical dash lines represents errors due to linear interpolation.

flux between including and excluding temperature data at 5 cm depth. It indicates that the result of TDEC is not sensitive to the data availability in the topsoil at either Anduo site or the twin-experiment, while LINEAR shows high sensitivity.

In studies on land-atmospheric interactions, surface energy closure ratio is an important index in the assessment of data quality and thus its estimation is important. The surface energy budget can be expressed below:

$$R_{net} = H + lE + G_0, \qquad (12)$$

where $R_{net}(\mathrm{W \cdot m^{-2}})$ is the net radiation, $H(\mathrm{W \cdot m^{-2}})$ the sensible heat flux, $lE(\mathrm{W \cdot m^{-2}})$ the latent heat flux, and $G_0(\mathrm{W \cdot m^{-2}})$ the surface soil heat flux.

Again, we analyzed the Anduo case. Table 2 shows monthly-mean surface energy budget, respectively, for $G_0>0$ (daytime) and $G_0<0$ (nighttime). Net radiation and turbulent fluxes were directly measured. Soil heat fluxes were calculated, respectively, by TDEC and LINEAR.

According to Table 2, when data at 5 cm depth was used, the unclosed energy ($\Delta E$) with LINEAR-derived $G_0$ is less than that with TDEC-derived $G_0$ in the case of

$G_0>0$, but larger in the case of $G_0<0$. The difference between the two methods is around 10%. However, when data at 5 cm depth were excluded, the unclosed energy between the two methods is greatly different. Therefore, the method for calculating soil heat flux and the data availability can have a great impact on the estimates of energy closure ratio, which should be emphasized in ABL studies.

**Table 2** Monthly-mean surface energy budget for $G_0>0$ (daytime) and $G_0<0$ (nighttime) at Anduo site[a]

|  | $R_{net}$ | $H$ | $lE$ | $G_0$ | $\Delta E$ |
|---|---|---|---|---|---|
| $G_0>0$ with 5 cm temperature data |  |  |  |  |  |
| LINEAR | 393 | 59 | 96 | 171 | 67 |
| TDEC | 392 | 59 | 96 | 157 | 80 |
| $G_0<0$ with 5 cm temperature data |  |  |  |  |  |
| LINEAR | −12 | −1 | 10 | −89 | 68 |
| TDEC | −13 | −1 | 10 | −82 | 61 |
| $G_0>0$ without 5 cm temperature data |  |  |  |  |  |
| LINEAR | 370 | 55 | 89 | 199 | 27 |
| TDEC | 392 | 59 | 96 | 155 | 81 |
| $G_0<0$ without 5 cm temperature data |  |  |  |  |  |
| LINEAR | 3 | 2 | 14 | −102 | 88 |
| TDEC | −14 | −1 | 9 | −83 | 60 |

a) $R_{net}$, $H$, and $lE$ are directly measured fluxes, and $G_0$ was calculated by TDEC or LINEAR. $\Delta E=R_{net}-(H+lE+G_0)$. Unit: $\mathrm{W \cdot m^{-2}}$.

## 5 Conclusions

To construct the soil temperature profile from limited observations is crucial for estimating soil heat flux. This paper presents a new method, which uses TDE to construct the major part of soil temperature profile and a linear interpolation to correct minor errors of TDE solution, and then, integrates temperature profile to obtain soil heat fluxes at each soil depth (source code is available at a webpage[1]). The new method does not require
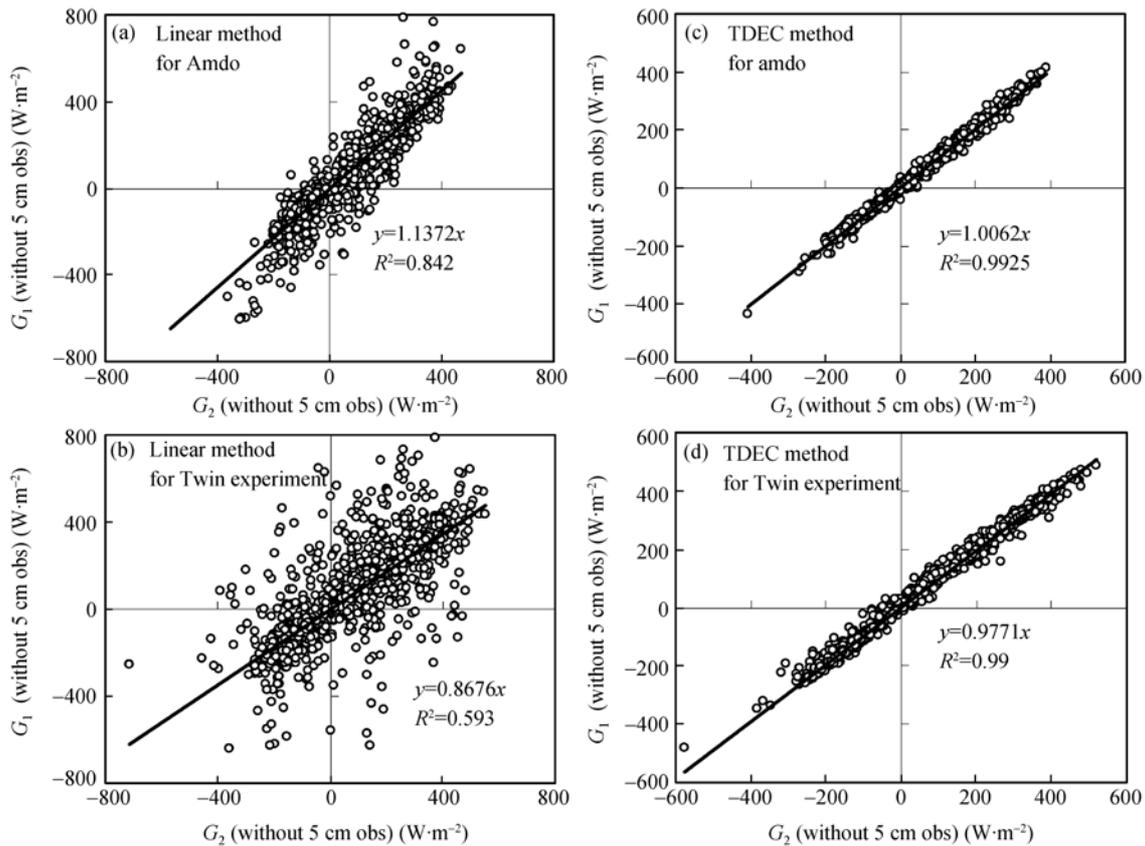
1) http://www.itpcas.ac.cn/users/YangKun/English.htm.

**Figure 8** Comparisons of soil heat fluxes, after giving different observations (X-axis: excluding 5 cm observations; Y-axis: including 5 cm observations). In (a) and (b), heat flux was derived with LINEAR. In (c) and (d), heat flux was derived with TDEC. (a), (c) At Anduo site; (b), (d) for the twin-experiment.

prior knowledge of soil thermal conductivity (or diffusivity). Besides, the results are not very sensitive to the data availability in the topsoil. The heat flux from this method was validated through a twin-experiment and its phase was validated with heat-plate measurements. This method can be applied to surface energy budget analyses in ABL experiments[19]. In addition, we pointed out that heat-plate measured soil heat fluxes cannot be directly used for estimating surface energy budget, and its magnitude also needs corrections.

Finally, it is reminded that our method is not suitable to the estimation of deep soil heat flux, as it is neglected in the new method.

1  Bhumralkar C M. Numerical Experiments on the computation of ground temperature in an atmospheric general circulation model. J Appl Meteor, 1975, 14: 1246−1258[DOI]

2  Heusinkveld B G, Jacobs A F G, Holtslag A A M, et al. Surface energy balance closure in an arid region: Role of soil heat flux. Agric For Meteorol, 2004, 122(1-2): 21−37[DOI]

3  Tanaka K, Ishikawa H, Hayashi T, et al. Surface energy budget at Amdo on the Tibetan Plateau using GAME/Tibet IOP98 data. J Meteorol Soc Jpn, 2001, 79(1B): 505−517[DOI]

4  Li C, Duan T, Chen L, et al. Calculation of the soil heat exchange in Qinghal-Tibet Plateau. J Chengdu Inst Meteorol (in Chinese), 1999, 14(2): 129−138

5  Horton R, Wierenga P J, Nielsen D R. Evaluation of methods for determining the apparent thermal diffusivity of soll near the surface. Soil Sci Soc Am J, 1983, 47: 25−32

6  Mo X, Li H, Liu S, et al. Estimating of the soil thermal conductivity and heat flux in near surface layer from soil temperature. Chin J Eco Agric (in Chinese), 2002, 10(1): 62−64

7  Fan X, Tang M. A preliminary study on conductive and convective soil heat flux. Plat Meteorol (in Chinese), 1994, 13(1): 14−19

8  Gao Z, Fan X, Bian L. An analytical solution to one-dimensional thermal conduction-convection in soil. Soil Sci, 2003, 168(2): 99−107[DOI]

9  Gao Z. Determination of soil heat flux in a Tibetan short-grass prairie.

Bound-Layer Meteorol, 2005, 114: 165－178[DOI]

10  Ma Y, Su Z, Li Z L, et al. Determination of regional net radiation and soil heat flux densities over heterogeneous landscape of the Tibetan Plateau. Hydrol Proc, 2002, 16(15): 2963－2971[DOI]

11  Zhang L, Jiang H, Li L. Study of calculation of soil heat conduction: Progress and prospect. J Glaciol Geocryol (in Chinese), 2004, 26(5): 569－575

12  Dong W, Tang M. Preliminary results of mean soil heat flux calculated by soil temperature data observed at meteorological stations. Plateau Meteorol, 1992, 11(2): 115－125.

13  Sellers P J, Randall D A, Collatz G J, et al. A revised land surface parameterization (SiB2) for atmospheric GCMs. Part I: Model formulation. J Clim, 1996, 9: 676－705[DOI]

14  Oleson K W, Dai Y, Bonan G, et al. Technical Description of the Community Land Model (CLM). NCAR Technical Note, NCAR/TN-461+STR. 2004

15  Ogée J, Lamaud E, Brunet Y, et al. A long-term study of soil heat flux under a forest canopy. Agric For Meteorol, 2001, 106: 173－186[DOI]

16  Koike T, Yasunari T, Wang J, et al. GAME-Tibet IOP summary report. In: Numaguti A, Liu L, Tian L, eds. Proceedings of the 1st International Workshop on GAME-Tibet,1999 January 11－13, Xi'an. Tokyo: Japan Soc of Snow and Ice, 1999. 1－2

17  Yang K, Koike T, Fujii H, et al. Improvement of surface flux with a turbulence-related length. Q J R Meteorol Soc, 2002, 128: 2073－2087[DOI]

18  Yang K, Koike T, Yang D. Surface flux parameterization in the Tibetan Plateau. Bound-Layer Meteorol, 2003, 106: 245－262[DOI]

19  Yang K, Koike T, Ishikawa H, et al. Analysis of the surface energy budget at a site of GAME/Tibet using a single-source model. J Meteorol Soc Jpn, 2004, 82: 131－153[DOI]

20  Hu H P, Ye B S, Zhou Y H, et al. A land surface model incorporated with soil freeze/thaw and its application in GAME/Tibet. Sci China Ser D-Earth Sci, 2006, 49(12): 1311－1322

21  Yang K, Koike T, Ye B, et al. Inverse analysis of the role of soil vertical heterogeneity in controlling surface soil state and energy partition. J Geophys Res, 2005, 110: D08101, doi:10.1029/2004JD005500

22  Philip J R. The theory of heat flux meters. J Geophys Res, 1961, 66: 571－579

23  Van Loon W K P, Bastings H M H, Moors E J. Calibration of soil heat flux sensors. Agric For Meteorol, 1998, 92(1): 1－8[DOI]